scientific reports

Check for updates

OPEN

Preparation of biocompatible Zein/Gelatin/Chitosan/PVA based nanofibers loaded with vitamin E-TPGS via dual-opposite electrospinning method

Homa Hodaei[1], Zahra Esmaeili[2], Yousef Erfani[3], Seyedeh Sara Esnaashari[1]✉, Mahvash Geravand[2] & Mahdi Adabi[2,4]✉

Wound management is a critical aspect of healthcare, necessitating effective and innovative wound dressing materials. Many existing wound dressings lack effectiveness and exhibit limitations, including poor antimicrobial activity, toxicity, inadequate moisture regulation, and weak mechanical performance. The aim of this study is to develop a natural-based nanofibrous structure that possesses desirable characteristics for use as a wound dressing. The chemical analysis confirmed the successful creation of Zein (Ze) (25% w/v) /gelatin (Gel) (10% w/v) /chitosan (CS) (2% w/v) /Polyvinyl alcohol (PVA) (10% w/v) nanofibrous scaffolds loaded with vitamin E tocopheryl polyethylene glycol succinate (Vit E). The swelling percentages of nanofiber (NF), NF + Vit E, cross-linked nanofiber (CNF), and CNF + Vit E were 49%, 110%, 410%, and 676%, respectively; and the degradation rates of NF, NF + Vit E, CNF, and CNF + Vit E were 29.57 ± 5.06%, 33.78 ± 7.8%, 14.03 ± 7.52%, 43 ± 6.27%, respectively. The antibacterial properties demonstrated that CNF impregnated with antibiotics reduced *Escherichia coli (E. coli)* counts by approximately 27–28% and *Staphylococcus aureus (S. aureus)* counts by about 34–35% compared to negative control. In conclusion, cross-linked Ze/Gel/CS/PVA nanofibrous scaffolds loaded with Vit E have potential as suitable wound dressing materials because environmentally friendly materials contribute to sustainable wound care and controlled degradation ensures wound dressings breakdown harmlessly.

Keywords Zein, Chitosan, Nanofibers, Electrospinning, Gelatin

The human skin, the largest organ, sustains humans' body from external pathogens. However, it can be injured from various factors, such as mechanical forces and chemical agents. The reparative process of cutaneous injuries entails four distinct phases: hemostasis, inflammation, proliferation, and regeneration[1]. The process of wound healing occurs through the intrinsic ability of the skin to regenerate independently, but this process may be extended due to microbial infection. Infected wounds create obstacles in the natural healing process and cause tissue deformation and significant pain for patients[2].

In wound healing management, wound dressings are crucial as they shield the wound from foreign agents and accelerate the treatment process. In the process of wound care, an effective dressing material must be able to remove exudate and protect the wound site. An ideal wound dressing material should possess high porosity to facilitate proper gas exchange while providing a reliable barrier against infection and dehydration[3].

Electrospun NFs present a promising option for wound dressing applications, with numerous possibilities among feasible candidates. The electrospinning method is flexible, relatively simple, cost-effective, and scalable, and also it has the capability to generate a structure that imitates the extracellular matrix (ECM)[4]. By adjusting

[1]Department of Medical Nanotechnology, Faculty of Advanced Sciences and Technology, Tehran Medical Sciences, Islamic Azad University, Tehran, Iran. [2]Department of Medical Nanotechnology, School of Advanced Technologies in Medicine, Tehran University of Medical Sciences, Tehran, Iran. [3]Department of Medical Laboratory Sciences, School of Allied Medical Sciences, Tehran University of Medical Sciences, Tehran, Iran. [4]Food Microbiology Research Center, Tehran University of Medical Sciences, Tehran, Iran. ✉email: s.esnaashari@iautmu.ac.ir; madabi@tums.ac.ir

the size and porosity of the electrospun mats, microorganisms can be prevented from penetrating while allowing oxygen to reach the wound site more easily[5]. NFs possess a vast surface area, which renders them higher drug loading and a sustained release behavior. This is accomplished by adsorbing intended drugs or bioactive molecules onto their surface or encapsulating them within their matrix[6]. A plethora of synthetic, natural polymers, and combination of both of them have been employed in the production of electrospun NFs as wound dressing[7]. CS, a natural polymer obtained from chitin deacetylation, possesses several valuable features such as biodegradability, biocompatibility, anti-bacterial properties, the ability to mimic glycosaminoglycan (GAGs) found in the ECM, and also the hemostatic characteristics. These features have led to the numerous applications of CS electrospun NFs in tissue engineering[8,9]. During the initial period of wound healing, it has been shown that CS could stimulate the movement of polymorphonuclear neutrophils (PMNs), which leads to the granular appearance the tissue and collagen production by fibroblasts. Researchers have provided evidence of the beneficial effects of CS on granular layer regeneration and skin re-epithelialization[10]. However, its suboptimal mechanical features and rapid degradation rate can be eliminated by incorporating additional synthetic polymers such as PVA and implementing cross-linking[11]. PVA as a synthetic polymer exhibits numerous advantages including hydrophilicity, biocompatibility, biodegradability, and nontoxicity. These properties introduce PVA as an attractive material for use in tissue engineering and wound care[12]. Furthermore, the straightforward electrospinning of PVA makes it a suitable case to improve the electrospinability of natural polymers when utilizing the electrospinning technique[13]. Gel is a Food and Drug Administration (FDA) approved polymer, derives from collagen hydrolysis, which is biocompatible and biodegradable[14]. Fibronectin is one of the adhesive molecules, which plays important role in wound healing. It has attaching domains for native collagen, but its tendency is even more for Gel fibers compared to collagen. Thus, Gel can be used in wound dressing and also as cell scaffold[15]. Although Gel NFs have been electrospun successfully, it suffers from poor mechanical properties. Combining Gel with another protein polymer such as Ze could potentially enhance structural integrity of the dressing while maintaining breathability and flexibility. Ze, a biodegradable and biocompatible plant protein, has been utilized in fabricating and developing numerous substrates and films for biomedical applications[16]. This protein is founded in the endosperm of maize (Zea mays) in its amorphous form[17]. Ze possesses advantageous characteristics including flexibility, biodegradability, antioxidant activity, and biocompatibility, making it suitable for various fields such as food packaging, tissue engineering, drug delivery, and wound dressing[18,19].

Various therapeutic agents can be loaded into or on NFs structure. Vit E is an essential compound in skin regeneration due to recruiting collagen accumulation in wound area. It is usually applied locally in form of lotion, cream and ointment, but it may become ineffective due to degradation. Therefore, its derivates are used[20]. A hydrophilic type of Vit E is D-α-tocopherol polyethylene glycol 1000 succinate (Vit E-TPGS) with powerful skin regenerative, antioxidant and anti-inflammatory activity, while it has low cost and high availability[21]. Vit E-TPGS can be hydrolyzed within intracellular milieus and released α-tocopherol[20]. Electrospun NFs mat containing Vit E-TPGS can deliver this vitamin efficiently to the wound area during healing process. While the incorporation of vitamins such as Vit E into electrospun NFs has been previously studied[20,22], the complex structure of Ze, Gel, CS and PVA electrospun NFs containing Vit E has not been reported, yet. Our study investigates the preparation of nanofibers using a blend of Ze, Gel, CS, and PVA, loaded with vitamin E through a dual-opposite electrospinning method. Defrates et al.[23] explored the application of Ze NFs in drug delivery, demonstrating their ability to effectively encapsulate and release drugs in a controlled manner. Ferreira et al.[24] examined Gel/CS NFs doped with phlorotannin-enriched extract for wound dressing, highlighting their antimicrobial properties without toxicity, which promotes wound healing. Zahra et al.[25] focused on electrospun PVA nanofibers for drug delivery. They concluded when PVA is blended with other polymers, particularly CS, the crosslinking of the fibers is an important factor which can affect the drug release characteristics of the fiber mats. Our work explores an innovative, nanofibrous wound dressing scaffold made from natural materials with a net-like structure through a double-nozzle electrospinning technique. The scaffold's performance is improved by cross-linking, which increases its water absorption capacity and decreases the degradation rate while also demonstrating significant antibacterial activity against various bacteria. Thus, Ze in combination with Gel and CS in combination with PVA were electrospun in a double nozzles system, while Vit E-TPGS was loaded in CS/PVA solution. Vit E solubility in Gel may limit efficient encapsulation. However, PVA/CS NFs offer better compatibility for Vit E loading. Physiochemical, haemolytic, antibacterial and biocompatibility evaluation of the resulting nanofibrous mat was performed to appraise its potential for wound dressing.

Methods and materials

Materials

CS (medium molecular weight), PVA (M_n = 70 000), Type B Gel, Ze, Phosphate buffered saline (PBS) and MTT [3-(4,5-dimethylthiazol-2-yi)-2,5-diphenyltetrazolium bromide] were obtained from Sigma-Aldrich (St. Louis, USA). Vit E was bought from Shaanxi Guanjie Technology Co., Ltd. (China). Glutaraldehyde (GA) and acetic acid were supplied from Merck company. *E. coli* (ATTC 25922) and *S. aureus* (ATCC 25923) strains were used as Gram-negative and Gram-positive bacterial strain, respectively. The NIH 3T3, mouse embryonic fibroblast cells, was provided from cell bank of Pasteur Institute of Iran.

Solutions preparation

Ze/Gel solution

This study obtained blended solutions by dissolving predetermined amounts of Gel and Ze in 80% (v/v) acetic acid at protein concentrations of 30%, 35%, and 40% (w/v). The weight ratios utilized were 10:20 (for 30%), 10:25 (for 35%), and 15:25 (for 40%) (Gel to Ze). The solutions were stirred for 24 h at 25 °C with a magnetic stirrer operating at a speed of 600 rpm.

CS /PVA solutions
A 10% (w/v) PVA solution was prepared by solubilizing PVA in distilled water with a magnetic stirrer for 2 h at 70 °C and a rotational speed of 600 rpm. The varying concentrations of CS solution (0.5%, 1%, 1.5%, and 2% w/v) were prepared in a 2% acetic acid solution on a magnetic stirrer at room temperature for 24 h with 200 rpm rate. Subsequently, the blended solution with a final concentration of CS (2% w/v) and PVA (10% w/v) was prepared using a volume ratio of 70:30 (CS/PVA) and stirred at room temperature for 30 min with 400 rpm speed.

PVA/CS/Vit E solution
Based on preliminary study, the optimized CS/PVA solution was selected for blending with Vit E. Specifically, 0.1 gr of Vit E was dissolved in 10% w/v PVA solution on a magnetic stirrer at room temperature for 30 min at 200 rpm. Then, the resulting PVA/Vit E solution was combined with CS in the optimal weight ratio, and the final mixture was placed at 30 °C to eliminate any remaining bubbles.

Electrospinning process
To produce NFs, a dual-opposite-spinneret electrospinning device called Electroris manufactured by Fanavaran Nano Meghyas Ltd., Co., (Tehran, Iran) was used. The device had two separate sets of syringe pumps and high voltage supplies. Prepared solutions were filled into the two 5 mL plastic syringes with 18 gauge metallic blunt-ended needles made of stainless-steel as nozzles. The first set was used to inject Ze/Gel. At the same time, electrospinning was performed at a voltage of 17 kV, flow rate of 0.5 mL/h, and a distance of 150 mm between the alumina foil collector and needle tip. Simultaneously, CS/PVA/Vit E solution was injected through the opposite nozzle and electrospun at a voltage of 20 kV, a solution feeding rate of 0.5 mL/h, and a distance of 150 mm between the alumina foil collector and needle tip. The electrospinning process was carried out for about 4 h, and finally, Ze/Gel/CS/PVA/Vit E nanofibrous mat (NF + Vit E) was obtained. The most suitable fibers were obtained from a 70:30 for CS (2% w/v) to PVA (10% w/v)(and 25:10 (35% w/v)for Ze to Gel, respectively.

The cross-linking process of NF
The cross-linking process of NFs was conducted with Glutaraldehyde 25% (GA) to increase the stability of NFs. The nanofibrous mats underwent a treatment process involving exposure to GA vapor in a sealed chamber for 24 h at ambient temperature. The cross-linked mats were subsequently rinsed with water to ensure all traces of GA were removed, making them suitable for further use.

Characterization of morphology
Scanning electron microscopy (SEM) (XL30 model), a product of Philips, Netherlands, operated at an accelerating voltage of 25 kV, was applied to investigate the diameters and morphology of the produced NFs. Prior to scanning, gold sputter coating was used to all samples. The Image J software was utilized to randomly measure 20 fibers diameter per image to determine the fibers mean diameter. Furthermore, a graph illustrating the fibers diameter distribution of each sample was generated using R software 4.3.0 version.

Fourier Transform Infrared spectroscopy (FTIR)
The NF specimens and the raw materials were subjected to chemical composition analysis through FTIR spectrometry, using the Thermo Fisher Scientific FTIR spectrometer model Nicolet iS10.

Water uptake ratio
The water uptake of the specimens was evaluated by cutting them into 1×1 cm^2, weighing them and submerging them in a PBS solution with a pH of 7.4 at 37 °C for 24 h. The samples were dried using filter paper and weighed on a digital scale to determine their wet weight. Then, the percentage of water uptake was calculated by Eq. [1].

$$(WC) = \frac{W - W_0}{W_0} \times 100 \tag{1}$$

In this regard, W is equivalent to the wet weight of the fiber, and W_0 is equivalent to the dry weight of the fiber.

Degradation of NF
In order to assess the degradation of electrospun NFs, a 1×1 cm^2 sample was weighed (W_0) and subsequently immersed in a buffer solution at 37 °C. After an incubation period of 24 h, the sample was extracted from the solution and allowed to dry for an additional 48 h at room temperature. The weight of the sample after drying (W) was measured, and Eq. [2] was used to determine the weight loss percentage.

$$WL = \left[\frac{W_0 - W}{W}\right] \times 100 \tag{2}$$

Contact angle measurements
To quantify the hydrophilicity of NFs, contact angle measuring was utilized. The surface of the NF was subjected to a 1μL drop of distilled water. The static drop methodology and contact angle recording video system (CA-500 A) were employed. Image J contact angle plugin (Drop Analysis) was utilized for analyzing the drop images.

Mechanical test

The mechanical properties of CNF and CNF + Vit E scaffolds were evaluated using a Universal Testing Machine (Santam, Iran). The scaffolds were prepared for testing by cutting them into dimensions of 3 cm × 0.5 cm. Subsequently, they were securely fastened in the grips and subjected to stretching at a speed of 2 mm/min, utilizing a load cell with a capacity of 10 N. Each sample underwent three measurements of mechanical parameters, and the resulting stress-strain curves were meticulously documented.

Antibacterial assay with disc diffusion method and bacterial cell viability assay

The antibacterial efficacy of various electrospun nanofibrous mats was assessed using both the disc diffusion method and a quantitative bacterial cell viability assay[26,27]. Two bacterial strains, *Escherichia coli* (ATCC 25922) and *Staphylococcus aureus* (ATCC 25923), were used for this study.

Disc diffusion method

E. coli and *S. aureus* were incubated in Mueller-Hinton Agar (MHA) medium at 37 °C for 24 h. A bacterial suspension equivalent to 0.5 McFarland standard (approximately 1.5×10^8 CFU/mL) was prepared and cultured on MHA plates. Uniform NF pieces (10 mm diameter) were cut and sterilized with UV light for 30 min. Crosslinked NFs loaded with Vit E were immersed in 1% penicillin solution for 2 h to create antibiotic-containing NFs. These electrospun nanofibrous mats were placed on the bacterial-inoculated plates and incubated for 24 h at 37 °C. The zone of inhibition was measured in millimeters using a digital caliper. Each test was performed in triplicate.

Bacterial cell viability assay

For quantitative analysis, a bacterial cell viability assay was performed. Antibiotic-containing nanofibrous mats (1 cm^2) were placed in 24-well plates containing 1 mL of bacterial suspension (~1×10^8 CFU/mL) in Mueller-Hinton Broth (MHB). The plates were incubated at 37 °C for 24 h. After incubation, 100 µL of the medium was removed from each well and serially diluted in PBS. From each dilution, 100 µL was plated on MHA and incubated for 24 h at 37 °C. The viable bacteria were then quantified using the colony counting method. The results were expressed as log CFU/mL, and the percentage reduction in bacterial colonies was calculated using the following formula [3]:

$$\text{Percentage reduction} = \frac{\text{CFU control} - \text{CFU treated}}{\text{CFU control}} \times 100 \tag{3}$$

where CFU control is the number of colonies in the untreated sample and CFU treated is the number of colonies in the sample treated with nanofibrous mats.

MTT assay

The ISO 10993-5 standard test method was used to evaluate the biocompatibility of the CS/PVA/Gel/Ze/Vit E nanofibrous scaffolds by indirect method (extract method)[28]. For this purpose, the fibers were sterilized with UV light and incubated in a culture medium for a week at 37 °C to create extracts. In order to perform the MTT assay, NIH-3T3 mouse fibroblast cells were cultured at a density of 7000 cells per well in a medium supplemented with 10% fetal bovine serum (FBS) in 96-well plates. After 24 h incubation, the medium utilized for culturing was poured out. Then, 90 µL of the fiber extract and 10 µL of FBS were added to each well. After 24, 48, and 72 h, the viability of the cultured cells was quantified by the colorimetric MTT assay, and optical density (OD) detection at 540 nm was used based on ELISA Reader ELX 808.

Cell attachment assay

In order to assess the adherence of NIH-3T3 mouse fibroblast cells to electrospun CNF and CNF + Vit E were cut into circular sections and then sterilized using ultraviolet radiation for 45 min before being placed into a 6-well plate and submerged in a culture medium. After 24 h of incubation at 37 °C, fibroblast cells were added to each well at a concentration of 1×10^4 cells per well. The cell adhesion assay was conducted at 24-hour intervals. This was achieved by replacing the culture medium on the sample surface with a 2.5% GA solution to stabilize the cells that adhered to it. The samples were subsequently kept at a temperature of 4°C for 4 hours and then dehydrated in alcohol gradient solutions. The cultured cells on the NF surface were finally recognized by SEM.

Hemolysis assay

The hemolysis test was employed to assess the blood compatibility of NFs sample. The volunteers' blood samples were mixed with 3.8% sodium citrate in a 10:1 ratio to prevent coagulation, followed by dilution with normal saline in a 4:5 ratio. 0.5 mL of the diluted blood was added to NFs samples, which put into 24-well plates and incubated for 1 h at 37 °C. After that the resulting blood was centrifuged at 2000 rpm for 5 min in microtubes. The supernatant, positive control, and negative control were subjected to spectrophotometric measurement at a wavelength of 545 nm, and the percentage of hemolysis was calculated using the formula [4][29,30]:

$$\text{Blood Hemolysis Percentage} = \frac{\text{OD test} - \text{OD negative control}}{\text{OD positive control} - \text{OD negative control}} \times 100 \tag{4}$$

The positive control consisted of 0.2 mL of blood diluted in 10 mL of normal saline. In comparison, the negative control comprised a mixture of 0.2 mL of blood diluted in sodium citrate (0.1%) and normal saline (10 mL).

Ethics approval

All protocols were clarified and approved by the Ethics Committee of Tehran University of Medical Sciences (IR.TUMS.MEDICINE.REC.1401.441). Informed consent was obtained from all subjects. All experiments were performed in accordance with relevant guidelines and regulations.

Results

SEM microscopy was employed to investigate the diameter and morphology of electrospun NFs. The SEM images and the size distribution of CS/PVA electrospun NF (70:30 v/v) with various concentration of CS (0.5%, 1%, 1.5% and 2% w/v) mix with 10% w/v PVA solution were shown in Fig. 1. As demonstrated in Fig. 1, more concentrated CS solution led to smaller range of NF diameter. Consequently, the 2% w/v CS solution with 78 ± 19 nm diameter was selected. Since it had the tinniest diameter and also the highest CS concentration. Figure 2 shows that Ze/Gel created uniform and homogeneous electrospun NFs with minimum beads and droplets. Also, it shows the diameter range of Ze/Gel NF is from 284 to 658 nm. Ze (25% w/v) to Gel (10% w/v) is selected as the optimum mixture with a fiber diameter of 284 nm (Fig. 2).

Using GA vapor as a NF stability method did not cause significant changes in the morphology or random orientation of electrospun NFs. However, the average diameter of the NFs increased from 192 to 282 nm (Fig. 3).

The analysis of Fig. 4 reveals that an increase in the average diameter of NFs containing Vit E from 168 nm to 203 nm after vaporization with GA.

Chemical characterization of electrospun NFs

Figure 5 displays the FTIR analysis of the samples. The FTIR spectrum of CS exhibits CH stretching vibrations which are confirmed by the observed peak at 2916 cm^{-1} [31]. The broad peak observed at 3444 cm^{-1} corresponds to symmetrical vibrations of OH[31]. The band 1658 cm^{-1} is related to amide I band (C = O stretching) [32]. The FTIR spectra of pure PVA show the prominent peaks of absorption at four particular wavenumbers: 3441 cm^{-1}, 2919 cm^{-1}, and 1730 cm^{-1}, and, which is attributed to the OH stretching, CH stretching, and C=O stretching, respectively[33,34]. In Gel spectra, a broad absorption at approximately 3400 cm^{-1} was detected, corresponding to Amide A (O–H stretching and N–H vibration)[35,36]. The peak observed around 2919 cm^{-1} indicates C–H stretching vibration and peak at 1235 cm^{-1} appears due to Amide III (C–N stretching and N–H bending)[36–38]. The bands around 1650 cm^{-1} and 1550 cm^{-1} are related to Amid I (C = O stretching and N–H bending) and Amide II (N–H)[36,39]. The FTIR analysis of Ze shows the peaks about 3400 cm^{-1} are related to amide A (N-H, –OH bonds from amino acids in proteins). Peaks about 2919, 1650, and 1540 cm^{-1} are attributed to C–H stretching, amid I (C = O stretching) and amide II (N–H bending and C–N stretching vibrations)[40]. The FTIR analysis of Vit E shows peaks about 3325, 2900, 1740, and 1100 cm^{-1} which are related to O–H stretching, C–H stretching, C = O stretching, and C–O stretching, respectively[41,42]. The FTIR analysis of NFs shows peaks about 3303, 2930, 1650, 1527, and 1232 cm^{-1} which is attributed to amide A(N-H, –OH bonds), C–H stretching, amide I, amide II, and amide III. After crosslinking, the changes were not considerably in the shift and intensity of peaks compared to NFs. The reason may be due to the same functional groups GA with NFs. Similarly, Vit E loaded NF had no considerably changes in the shift and intensity of peaks compared to Vit E loaded CNFs. In addition, Vit E loaded NFs and Vit E loaded CNFs had an additional peak about 1739 cm^{-1} compared to NFs and CNFs, respectively, which confirm presence of Vit E into the NFs.

Water uptake ratio

Figure 6 illustrates that all stabilized (cross-linked) samples experienced significant water absorption. The swelling percentages of CNF, CNF + Vit E, NF, and NF + Vit E NFs were 676%, 410%, 110%, and 49%, respectively. The porous structure of the NF scaffolds facilitated the penetration of water molecules into the NF network. Among the NFs, CNF exhibited the highest percentage of water absorption.

Degradation of NF

According to the findings presented in Fig. 7, the homogeneous structure of the NFs displayed water resistance. It was observed that CNF had the highest capacity for water absorption and the lowest rate of degradation. The degradation rates of CNF, NF, CNF + Vit E, and NF + Vit E were $14.03 \pm 7.52\%$, $29.57 \pm 5.06\%$, $43 \pm 6.27\%$, and $33.78 \pm 7.8\%$, respectively. Cross-linking was found to make the NFs more resistant to degradation. At the same time, the addition of vitamin E was observed to increase their degradation rate, which might be due to the thinner diameter of NFs containing Vit E.

Contact angle measurement

Contact angle measurement is applied to investigate the hydrophilicity of prepared nanofibrous scaffolds. Considering the time-dependent nature of surface wettability, contact angles were measured for each sample at 0, 3, and 10 s. The resulting data are summarized in Table 1. The initial contact angle of CNF was found to be 118°, which decreased to 104° after 3 s. This was expected due to hydroxyl and amino groups on the NFs. Meanwhile, CNF + Vit E and NF + Vit E exhibited initial contact angles of 112° and 99°, respectively; after 3 s, these values decreased to 102° and 94°. However, it was observed that CNF, CNF + Vit E, and NF approximately absorbed the water drop after 10 s (Fig. 8).

Mechanical test

Our research has confirmed that the presence of Vit E could have an effect on the hydrophilicity properties of the fiber structure. Changes in water absorption may impact the physical properties of the films or fibers. Higher levels of moisture could lead to softening, resulting in a decrease in material rigidity and tensile strength. Furthermore, Vit E has the ability to cause structural irregularities, reduce the flexibility of polymer chains,

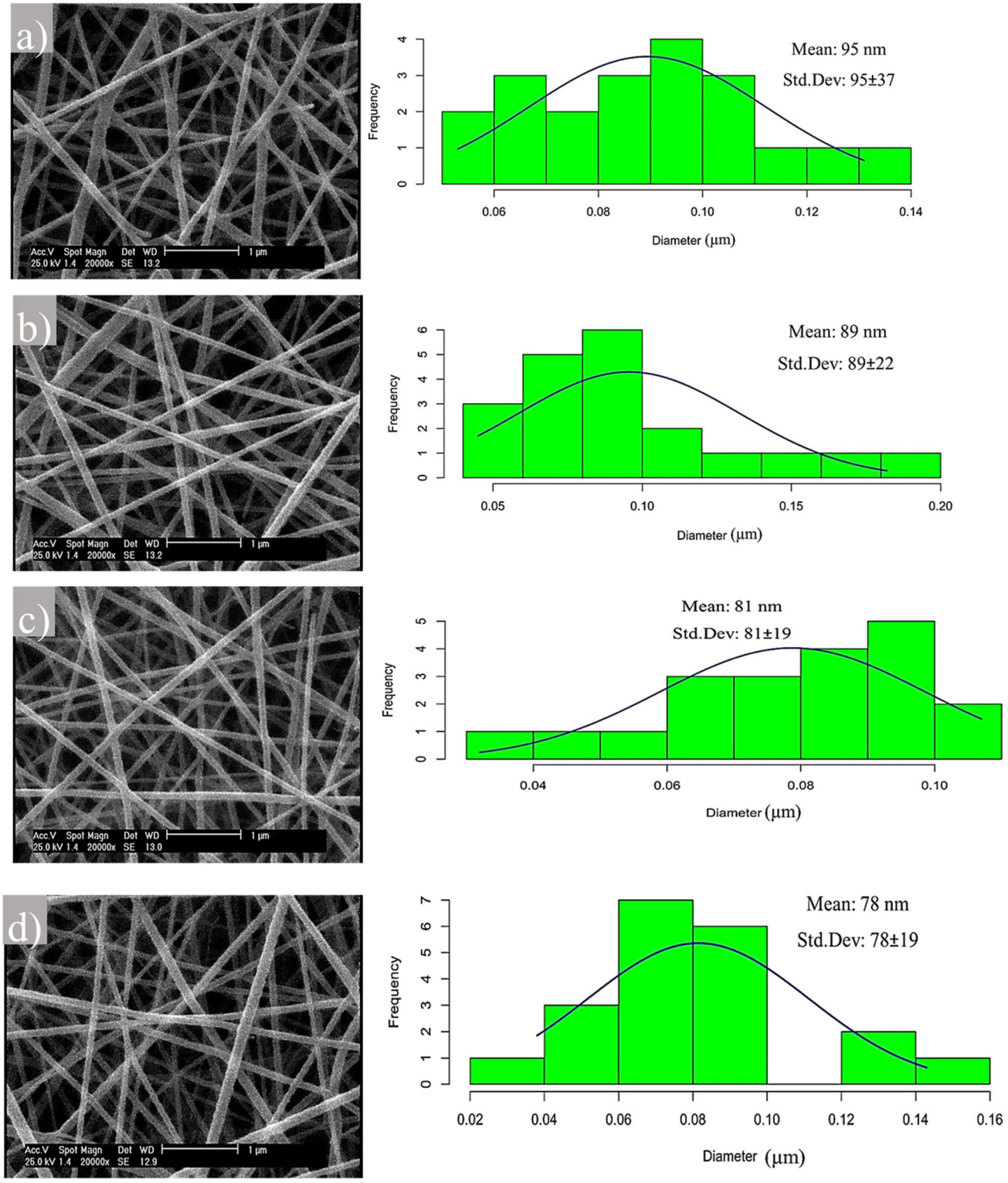

Fig. 1. SEM images and size distribution of electrospun NFs composed of CS/PVA (70:30 v/v) with different CS concentrations: (**a**) 0.5% w/v, (**b**) 1% w/v, (**c**) 1.5% w/v, and (**d**) 2% w/v mixed in a 10% w/v PVA solution.

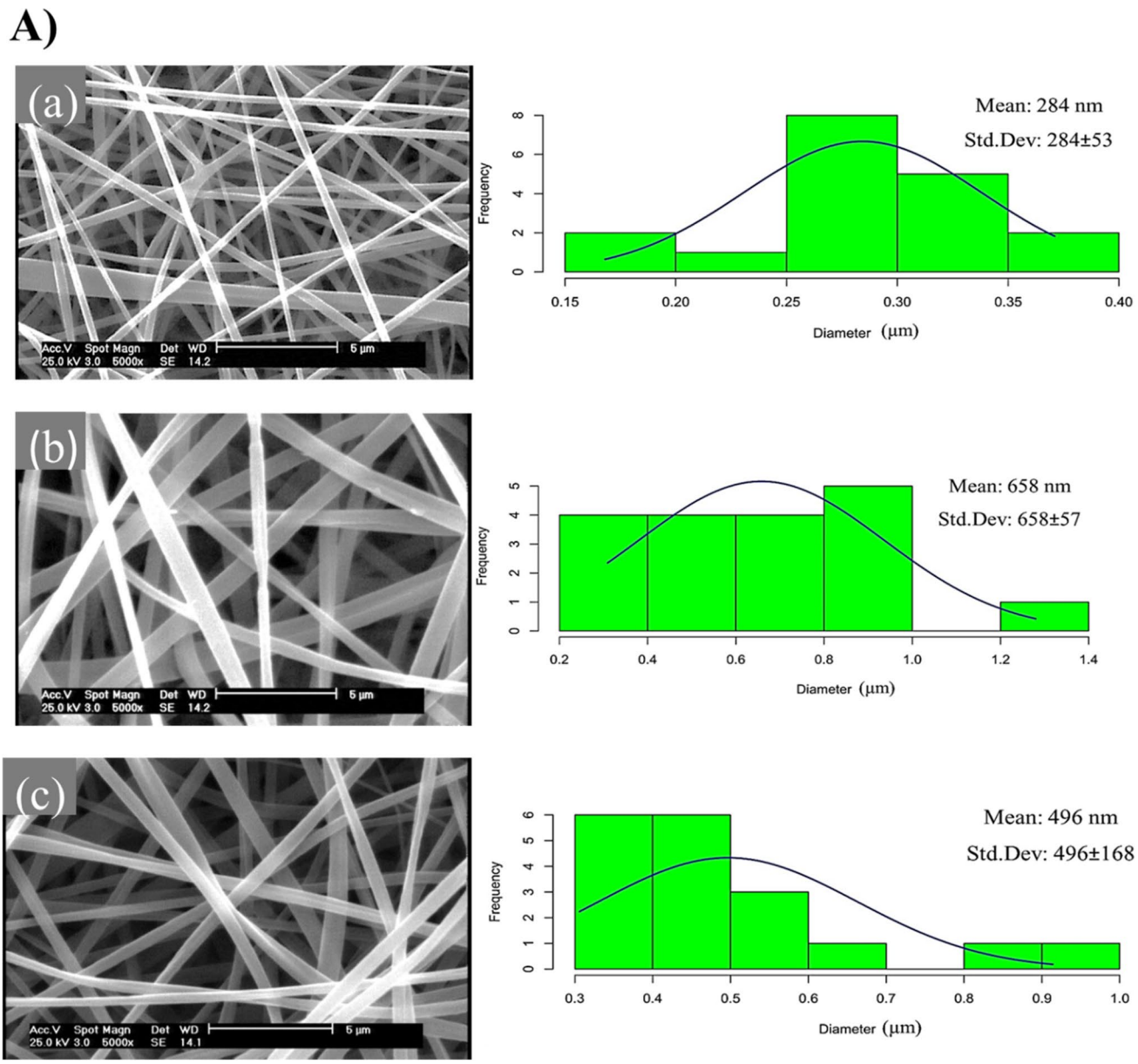

Fig. 2. SEM images and size distribution of electrospun NFs composed of Ze/Gel for different Ze/Gel concentrations: (**a**) Ze 25% w/v, Gel 10% w/v, (**b**) Ze 25% w/v, Gel 15% w/v, and (**c**) Ze 30% w/v, Gel 10% w/v.

and lower the water content in the films[43,44]. Consequently, our CNF containing vit E showed reduced tensile strength compared to CNF (Fig. 9). Also, the similar study[45] confirmed that increasing the amount of vitamin E in CS film resulted in reduced tensile strength.

Anti-bacterial activity

We evaluated the efficacy of electrospun nanofibrous mats using both the disc diffusion method and a quantitative bacterial cell viability assay against *E. coli* and *S. aureus* bacteria. The inhibitory effects of NFs on bacterial growth were assessed by measuring bacterial growth inhibition zones (Fig. 10; Table 2). Clear inhibition zones were observed for both bacterial strains, indicating the antibacterial properties of the NFs containing antibiotics (Penicillin). The quantitative analysis of antibacterial efficacy was performed using the CFU count method (Fig. 11). The results are expressed as log CFU/mL, demonstrating the effectiveness of the NFs in reducing bacterial populations. For *E. coli* and *S. aureus*, the bacterial counts after 24 h treatment and the percentage reduction in bacterial colonies are available in Table 2.

MTT assay

To assess the compatibility of the constructed scaffolds with skin fibroblast cells, a cell proliferation test was conducted at 24, 48, and 72 h. The survival outcomes of fibroblast proliferation for each group on the 1, 2, and 3 days are presented in Fig. 12. The results indicate that none of the groups had adverse effects on fibroblast

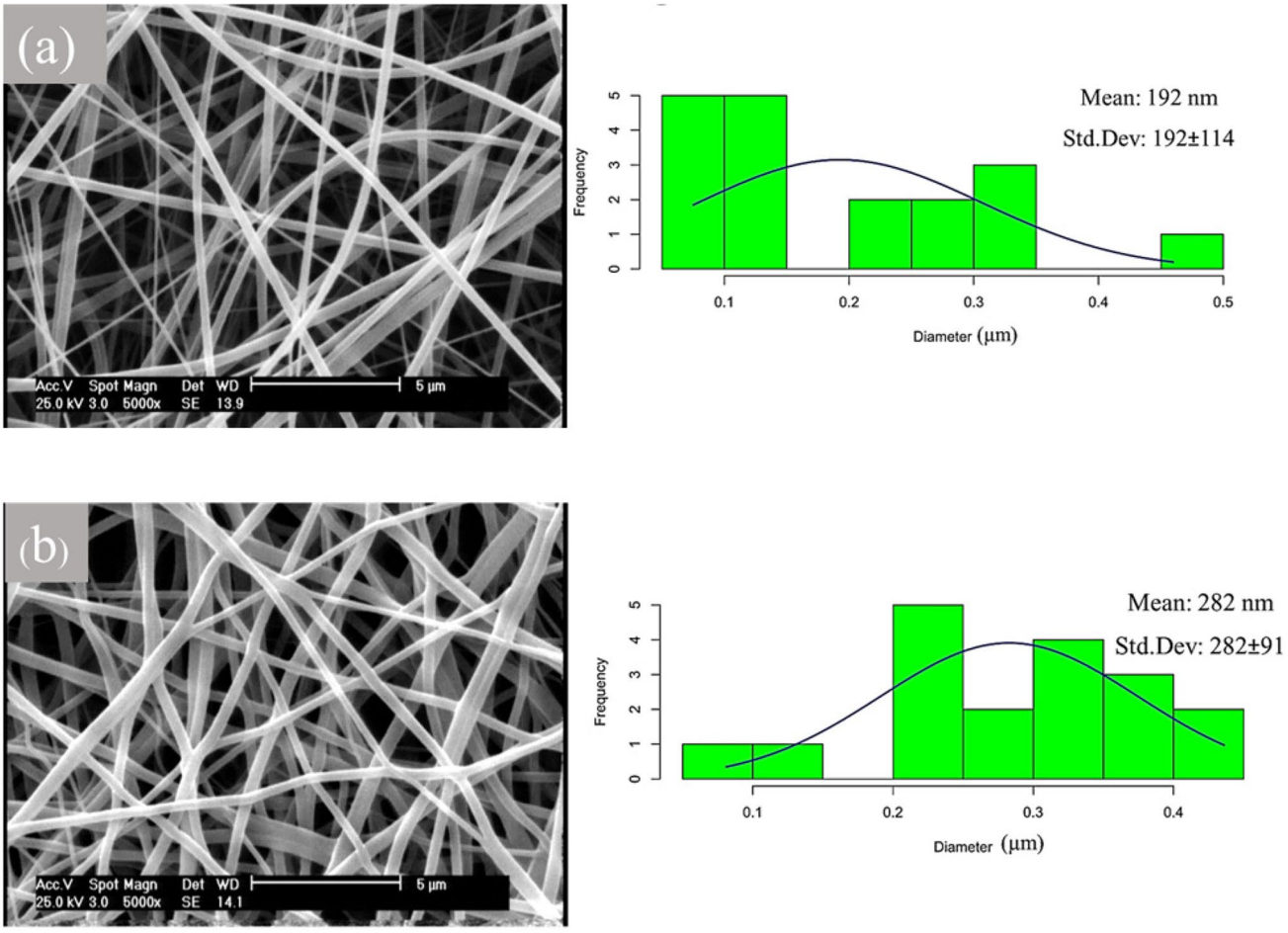

Fig. 3. SEM images and size distribution of electrospun NFs composed of (**a**) CS (2% w/v) /PVA (10% w/v) / Ze (25% w/v) / Gel (10% w/v); (**b**) cross-linked CS (2% w/v) /PVA (10% w/v) /Ze (25% w/v) /Gel (10% w/v).

proliferation, and no toxicity was observed during the testing period. Notably, NF + Vit E exhibited a relative increase in cell proliferation compared to other samples.

Cell adhesion on scaffolds

To assess the adherence of cells on scaffolding, the primary morphology of fibroblast cells in CNF + Vit E and CNF samples was evaluated using SEM. The fibroblast cells cultivated on CNF + Vit E and CNF displayed appropriate morphology and adhesion. Additionally, they interacted positively with adjacent NFs. (Fig. 13)

Hemolysis assay

Hemolysis is utilized to examine the response of red blood cells when exposed to external agents. Figure 14 depicts the hemolysis caused by NFs, revealing that all NFs exhibit minimal hemolysis (less than 1%). This outcome was expected due to the biocompatible polymers employed in the NFs fabrication process.

Discussion

The global need for wound care and treatment has surpassed the capabilities of conventional dressings due to their inadequate anti-bacterial properties and other shortcomings[46–48]. As a result, electrospinning technology has become increasingly popular among researchers as it offers a straightforward and flexible manufacturing approach. Electrospinning refers to a technique that utilizes voltage to create a fiber by stretching and elongating a jet formed from an electrified liquid droplet. In this process, the characteristics of produced NFs are influenced by both the properties of the polymer and solution, such as molecular concentration, conductivity, and molecular weight, as well as the specific electrospinning conditions used, including feeding rate, voltage, and distance between the collector and needle tip[49].

Electrospinning technology has the ability to generate nanofibrous wound dressings that provide numerous advantages in the medical domain. These dressings imitate the ECM structure and provide a surface for cellular attachment, proliferation, and differentiation[50]. Furthermore, this method can take advantage of both the natural polymers biocompatibility and the robust mechanical properties of synthetic polymers in a single process[51].

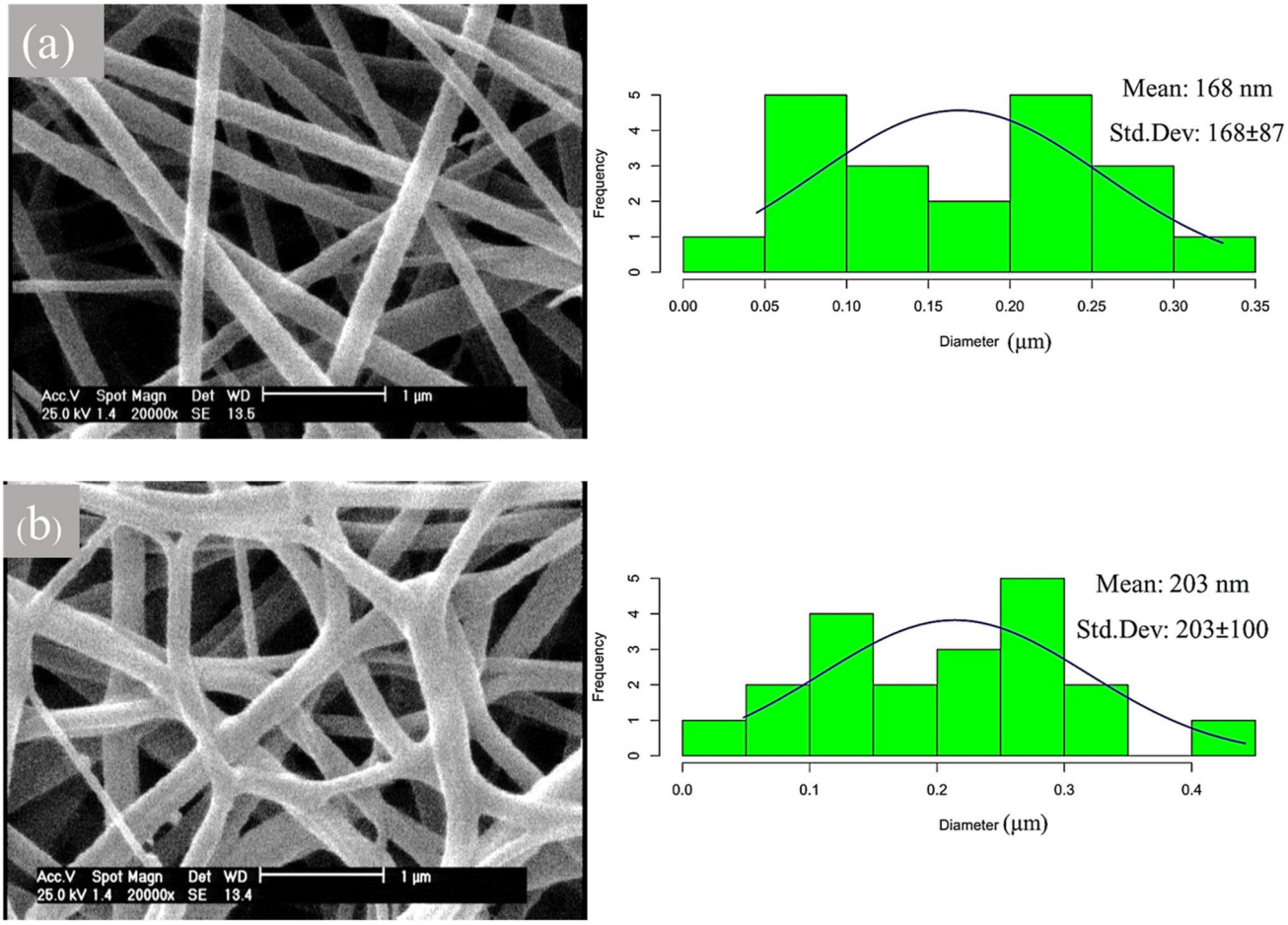

Fig. 4. SEM images and size distribution of electrospun NFs composed of (**a**) CS (2% w/v) /PVA (10% w/v) / Ze (25% w/v) / Gel (10% w/v) containing Vit E; (**b**) cross-linked CS (2% w/v) /PVA (10% w/v) /Ze (25% w/v) / Gel (10% w/v) containing Vit E.

The dual opposite electrospinning technique is favored for its unique ability to create a NF mat with different materials at the same time. By using a double nozzle system, Ze combined with Gel can be electrospun from one nozzle, while CS combined with PVA can be spun from the opposite nozzle. This method allows for the precise fabrication of a bilayered mat, where each layer has specific properties that can enhance the overall functionality of the wound dressing. In addition, it can produce more complex mats in a single step, reducing fabrication time and complexity. While Ze, Gel, and CS are soluble in acetic acid, their compatibility in a single blend may vary. PVA as a biocompatible and hydrophilic polymer, carries wound-healing agents and antimicrobials, making it crucial for skin-contact wound dressings and improve the mechanical properties.

The Electrospinning of pure CS and its derivatives into nanofibrous membranes demonstrates difficulty due to their polycationic nature and strong intramolecular forces[52,53]. To overcome this, the blending of CS with other polymers, like PVA[54] and polylactide (PLA), is recommended for preparing CS-based electrospun NFs[55]. Ohkawa et al. have demonstrated that blending CS with PVA can disrupt the formation of rigid associations between CS molecules. This owing to a strong hydrogen bonding interaction between the two polymers on a molecular level[56]. Additionally, PVA can be easily electrospun from an aqueous medium[57]. In this investigation, the combination of PVA and CS was chosen to enhance electrospinning proficiency, resulting in an augmentation of the hydrophilic nature of the nanofibrous structure. The SEM image of the mixed NF network containing CS and PVA with a 70:30 ratio revealed that the resulting NFs formed an interconnected network with uniform morphology and no beads. In a comparable investigation, CS/PVA NFs containing Ag NPs were produced through electrospinning with different volume ratios of 70:30 and 90:10 in 90% acetic acid with consistent electrospinning process parameters. A CS/PVA solution with a mass ratio 90:10 exhibited beaded structures. However, reducing the mass ratio of CS/PVA to 70:30 increased the electrical conductivity of the solution, resulting in the generation of the jet polymer during electrospinning and ultimately producing bead-free fibers[58].

The primary goal of this study was to create a composite electrospun NFs with biocompatible and antimicrobial properties, employing CS/PVA/Gel/Ze/Vit E for use in the dressing and wound covering industries. The GA vapor stabilization technique was employed to stabilize the NFs, widely studied among chemical methods. The outcomes revealed that the strength and stability of the NFs increased with GA crosslinking compared to the non-cross-linked NFs. SEM images of the non-cross-linked NFs depicted numerous holes on their surface, which

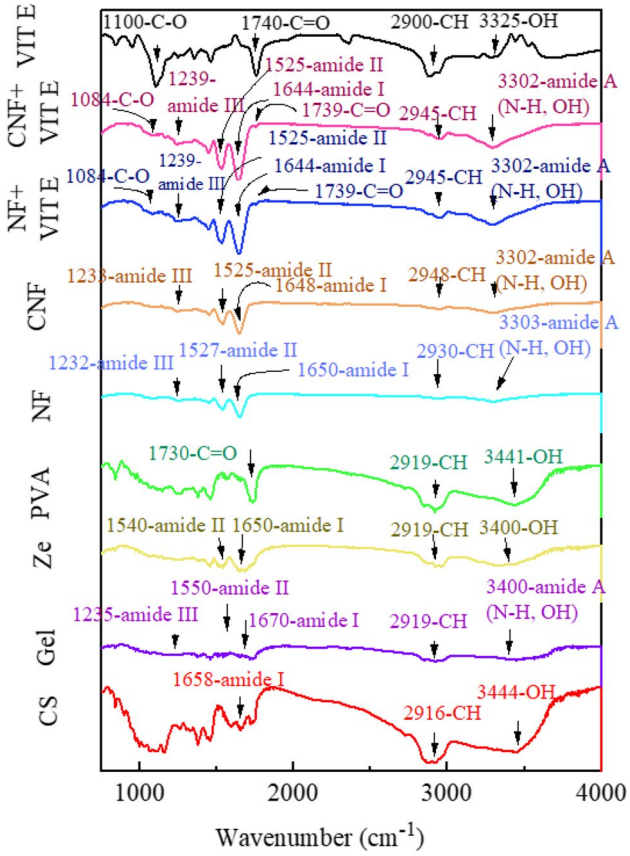

Fig. 5. The FTIR spectra of CS, PVA, Gel, Ze, NF, CNF, NF + Vit E and CNF + Vit E.

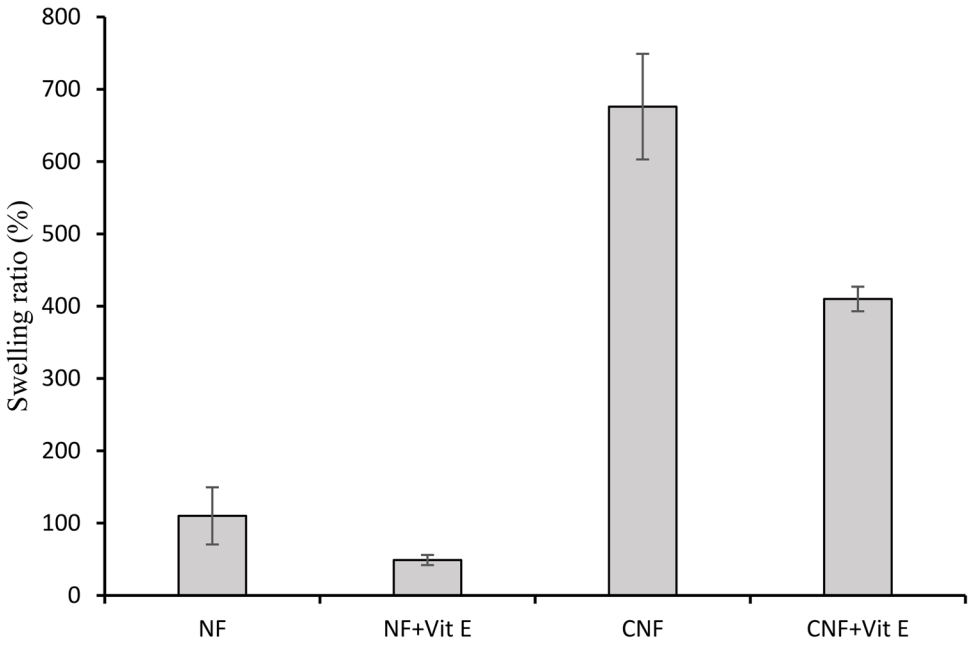

Fig. 6. The swelling ratio of NF, NF + Vit E, CNF and CNF + Vit E.

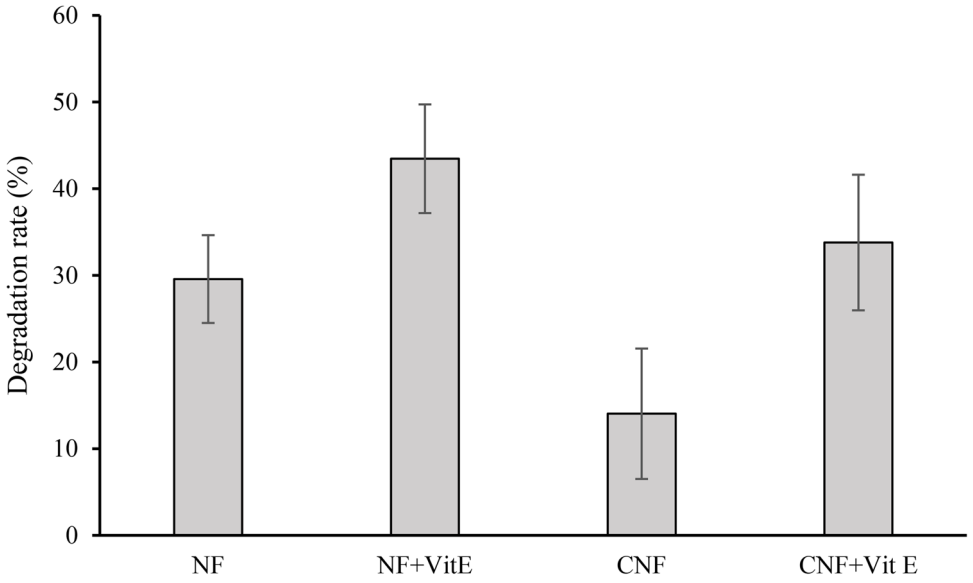

Fig. 7. The degradation ratio of NF, NF + Vit E, CNF and CNF + Vit E.

Samples	0 s	3 s	10 s
CNF	118°	104°	44°
CNF + Vit E	112°	102°	36°
NF + Vit E	99°	94°	26°

Table 1. Water contact angles of CNF, CNF + vit E, and NF + vit E after 0, 3, and 10 s.

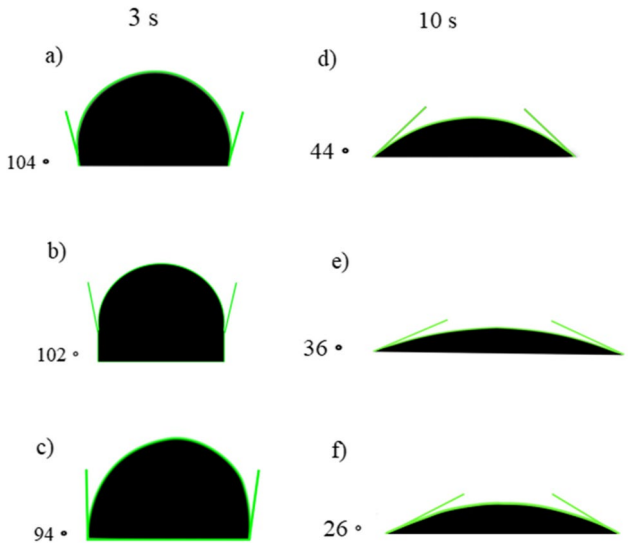

Fig. 8. Water contact angles of CNF, CNF + Vit E, and NF + Vit E after 3 and 10 s.

were significantly reduced upon GA addition, indicating an improvement in the strength of the NFs. Moreover, SEM images showed the presence of connection points between NFs in certain regions. The application of GA vapor for stabilization enhances these connection points, causing certain fibers to adhere to one another and augmenting their mechanical strength. Additionally, this process leads to an increase in the mean diameter of the NFs.

The quantitative bacterial cell viability assay results complemented the findings from the disc diffusion test, providing a precise measure of antibacterial efficacy. For *E. coli*, the log CFU/mL counts ranged from 7.12 to 7.22 for antibiotic-containing NFs, compared to 9.9 for the negative control—a reduction of approximately 27–28%.

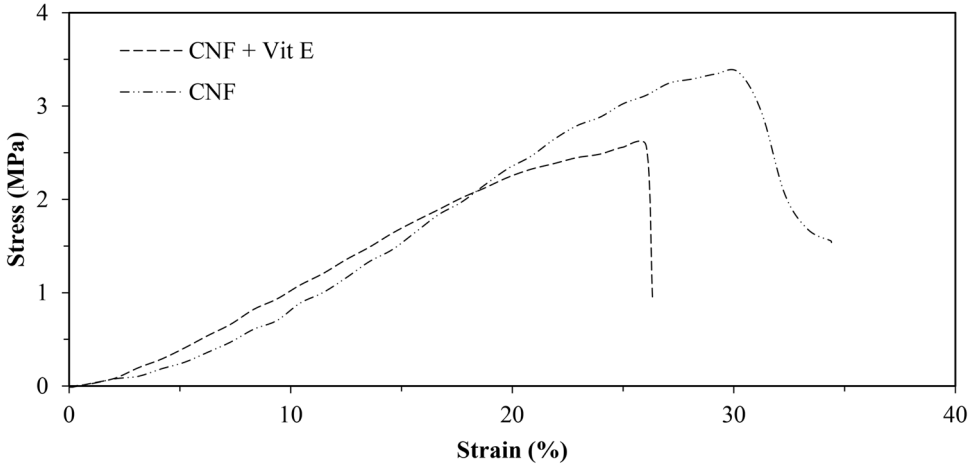

Fig. 9. Stress-strain curves of CNF and CNF + Vit E.

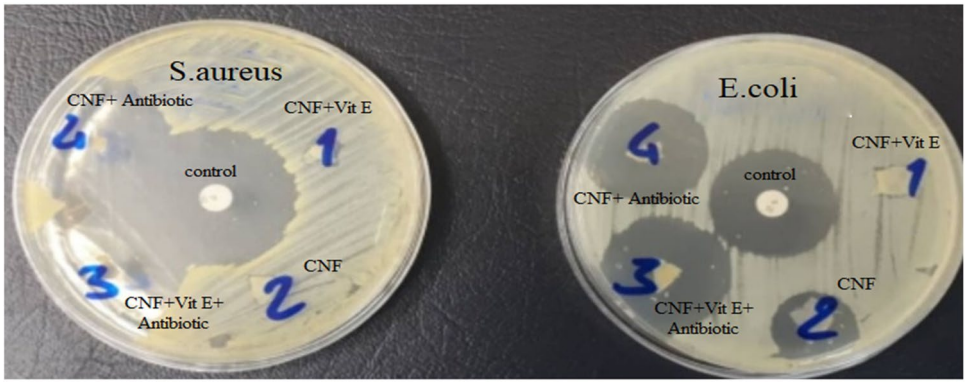

Fig. 10. The antibacterial inhibition area of CNF, CNF + Vit E, CNF + Antibiotic, and CNF + Vit E Antibiotic, and penicillin (positive control).

Sample	Inhibition zone (mm)		CFU count (log CFU/mL)		Reduction in Bacterial Colonies (%)	Reduction in Bacterial Colonies (%)
	E. coli	S. aureus	E. coli	S. aureus	E. coli	S. aureus
Negative control	-	-	9.9	9.9	-	-
CNF	19	-	7.9	9.9	20.2	No significant reduction
CNF + Vit E	-	-	9.9	9.9	No significant reduction	No significant reduction
CNF + Penicilline	26	34	7.22	6.45	27.1	34.8
CNF + Vit E + Penicilline	28	30	7.12	6.54	28.1	33.9
Penicilline (Positive control)	28	36	7.08	6.12	28.5	38.2

Table 2. The inhibition zone size of CNF + vit E, CNF, CNF + vit E + antibiotic, CNF + antibiotic, and penicillin (positive control) for *E. Coli* and *S. Aureus*.

Similarly, for *S. aureus*, the counts were 6.45 to 6.54 log CFU/mL for antibiotic-containing NFs, compared to 9.9 for the negative control, indicating a reduction of about 34–35%. Notably, *S. aureus* exhibited a greater reduction than *E. coli*, supporting the disc diffusion results and suggesting the NFs effectiveness against gram-positive bacteria. Interestingly, CNF alone showed a modest antibacterial effect against *E. coli* (20.2% reduction) but not against *S. aureus*. The combined use of qualitative (disc diffusion) and quantitative (CFU count) methods provides a comprehensive evaluation of antibacterial efficacy, as recommended by recent studies in antimicrobial biomaterials[26,59].

The stability of NF structures in aqueous environments is a crucial factor in creating effective scaffolds for wound healing, and in general, GA-vapor-stabilized NFs exhibited good stability after immersion in PBS. GA

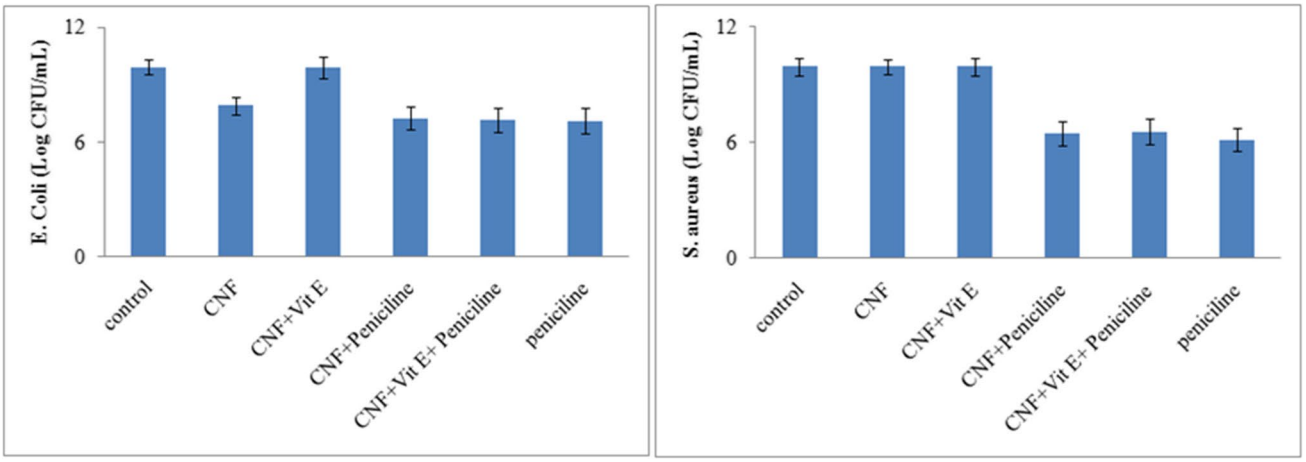

Fig. 11. The antibacterial CFU count of CNF, CNF + Vit E, CNF + Antibiotic, and CNF + Vit E Antibiotic, and penicillin (positive control).

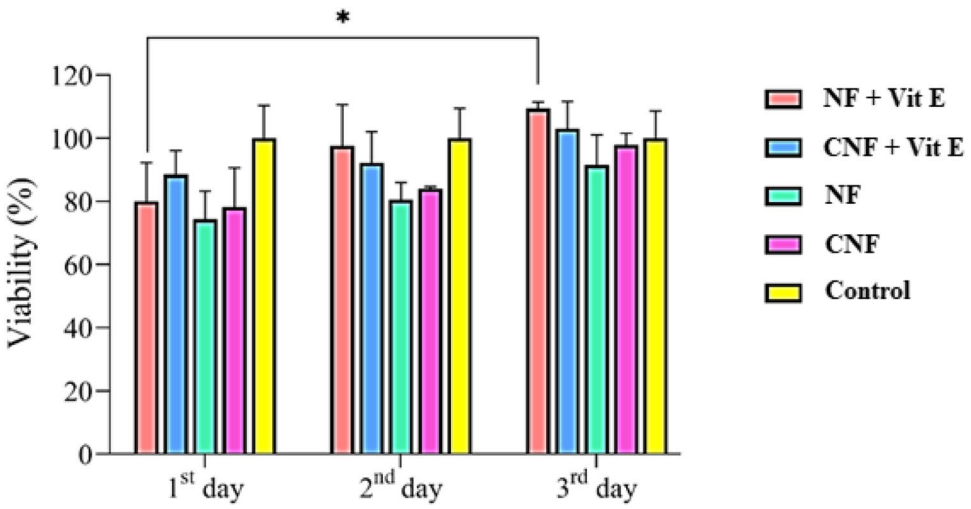

Fig. 12. The MTT assay of NIH-3T3 cell viability results of the NF + Vit E, CNF + Vit E, NF, CNF after 24, 48 and 72 h.

vapor cross-linking increased the average diameter (203 nm) of NFs containing Vit E compared to their initial diameter (168 nm) before vaporization.

The morphology of the produced layers was analyzed by SEM, revealing the formation of NFs that were free from defects. The results of FTIR, which indicated the bonding between the material components, corroborated the SEM findings.

The FTIR analysis effectively provided a characterization of different samples, highlighting the presence of key functional groups and their corresponding absorption peaks. The peaks associated with CS, PVA, Gel, Ze, Vit E, and NFs exhibited the diverse chemical functionalities within these materials. The stability observed in the FTIR spectra post-crosslinking indicated that the chemical structure of the nanofibers remains largely intact, suggesting effective crosslinking without significant alteration of functional groups. Additionally, the detection of an extra peak in the Vit E-loaded samples confirmed successful incorporation of Vit E, thereby increasing the functional properties of the NFs. Therefore, the findings underscore the utility of FTIR spectroscopy in clarifying the molecular composition and structural integrity of these materials, which is critical for their application in wound dressing and tissue engineering.

The electrospinning technique is subject to a range of parameters that affect the properties of the resulting NFs[60]. Figure 2 demonstrates the impact of the Gel to Ze ratio on NFs diameter distribution. The results suggest that a mixture containing 25% Ze and 15% Gel increases NF diameter. Based on morphological analyses, it can be inferred that a high proportion of Gel contributes to the formation of an assembled structure, resulting in a larger diameter for hybrid NFs. Lingli Deng et al. achieved similar results by utilizing hybrid electrospinning to create NFs consisting of Gel and Ze. Their findings indicated a significant augmentation in the diameter of Gel/Ze NFs with an increased ratio of Gel[14].

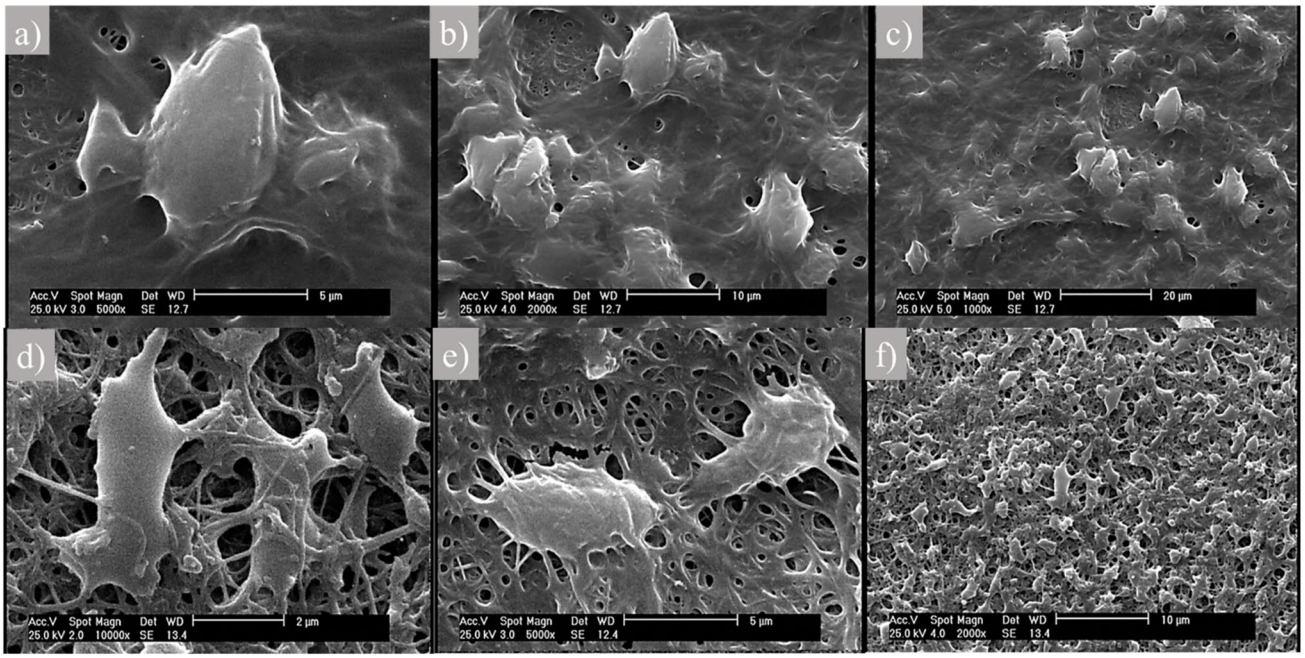

Fig. 13. SEM images of cultured fibroblast cells after 24 h of cell fixation at different magnifications (a - c) CNF (d - f) CNF + Vit E.

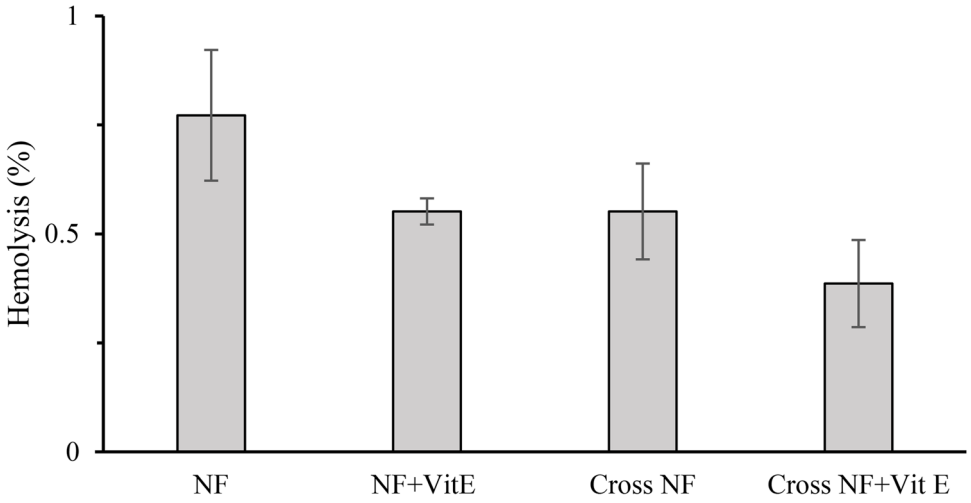

Fig. 14. Hemolysis test over the prepared samples.

The mechanical properties of NFs can decrease when they are loaded with Vit E due to several factors related to the interaction between the Vit E and the polymer matrix. The incorporation of Vit E may change the solubility and structural integrity of the polymer, disrupting intermolecular forces and resulting in decreased tensile strength and overall mechanical performance[61,62]. Additionally, Vit E can affect the molecular weight distribution of the polymer, resulting in a less cohesive structure and diminished mechanical strength. Specifically, the addition of Vit E can decrease the diameter of the NFs, affecting their load-bearing capacity[63]. Consequently, mechanical testing of NFs loaded with Vit E often shows decreased performance due to the Vit E effect on the polymer structural integrity, molecular interactions, and degradation behaviors, contributing to reduced tensile strength and overall mechanical stability.

The analysis of water absorption capacity and resulting graph demonstrate that NFs hydrophilic nature gives them a high moisture absorption capacity, making them suitable for wound secretion absorption. This swelling of NFs may be attributed to water molecule penetration within the NF networks. An essential factor of wound dressings is their ability to properly absorb secretions, preserve wound moisture, and prevent drying of damaged tissue surfaces[64]. Proper management of exudate prevent complications and promote tissue repair. Effective moisture absorption prevent maceration, which can soften and breakdown wound edges and surrounding

skin due to excessive moisture. In addition, absorbent dressings help maintain a clean wound environment by managing bacteria and debris in exudate.

The water absorption capacity of NFs significantly influences their degradation behavior. When NFs with high water absorption capacity encounter wound exudate or body fluids, they swell, leading to mechanical stress and gradual degradation. Swollen NFs exhibit an increased surface area, making them more accessible to enzymes. Proteases and other enzymes in wound environments break down NF polymers. Slowly degrading NFs are ideal for wound dressings, as they prevent negative effects of rapid degradation products on the wound. Balancing water absorption capacity is crucial to ensure NFs maintain integrity while promoting wound healing. Additionally, chemical crosslinkers like GA significantly reduce the rate of degradation of various biopolymers in both in vitro and in vivo aquatic environments[65]. crosslinking increases water resistance and decrease degradation by forming a stable network within the materials. This restricts water penetration and strengthens the structure.

The hydrophilicity of NF surfaces was evaluated in the current study by measuring the contact angle of water droplets at ambient temperature. The obtained angles were lower than 90 degrees, confirming the hydrophilic nature of the NFs expected from the existence of functional groups in the polymers.

Additionally, a previous investigation by Mirzaei et al. on CS-Gel/CS-hyaluronic acid NFs showed similar results, with all contact angles being below 90 degrees owing to the presence of polar groups in, Gel, hyaluronic acid, and CS that absorb significant amounts of water molecules, resulting in a decrease in contact angle and increased hydrophilicity on the NF surface[66]. In another study, the contact angles of pure CS and CS/Gel with different ratios were analyzed. The results indicated that CS/Gel NF mats exhibit higher hydrophilicity than pure CS NF mats, which can be attributed to the hydrophilicity of Gel[67]. According to the findings of Deng et al., when pure Gel film was exposed to water droplets, the droplets were immediately absorbed and lost their convex shape[14]. However, Wang et al. conducted a study where deionized water droplets on Gel/Ze NFs maintained a convex shape with a contact angle of 54.6°. This phenomenon was linked to the increased presence of hydrophobic groups in Ze and the formation of hydrogen bonds between Gel and Ze hydrophilic groups. They found out by increasing the amount of loaded perillaldehyde into Gel and Ze electrospun film, the hydrophilicity of the pure NFs was changed into hydrophobicity (from 54.6° to 141.5°). These interactions produced a hydrophobic surface for the Gel/Ze NF film[68]. Our research findings indicate that surfaces of the prepared CS/PVA/Gel/Ze nanofibrous mat had an acceptable hydrophilicity character, which facilitate cell attachment and proliferation. This aligns with previous studies which have highlighted the beneficial effects of moist environments in promoting healing and regeneration in damaged areas. Such environments promote the migration of fibroblasts, endothelial cells, and keratinocytes toward the wound location[69,70]. Providing appropriate conditions for cell proliferation is essential in promoting the healing process. As such, it is important to maintain a humid environment through the use of dressings with appropriate hydrophilicity[71]. In particular, NFs designed for wound dressing should be able to effectively absorb exudate from the injured site and prevent dehydration while limiting excess water vapor release[72].

In the field of wound care, wound dressings must exhibit a high degree of compatibility[7]. In order to assess the cytocompatibility of electrospun nanofibrous mats, an MTT assay was conducted with mouse fibroblast cells over a 1, 2, and 3 days. The NF + Vit E scaffold demonstrated more significant cell proliferation than other samples; this observed variation in cellular behavior may be attributed to differences in NF diameter between the treatments. Specifically, a decrease in NF diameter creates larger pore spaces between fibers, increasing specific surface area and thereby promoting the adhesion and proliferation of the cells[73]. Previous studies have established the influence of surface chemistry and NF diameter on cell proliferation on scaffolds[74,75]. Based on these findings, the developed nanofibrous scaffolds are highly biocompatible for tissue engineering applications. Zhou et al. conducted a study to fabricate poly (vinyl alcohol/carboxyethyl chitosan) (PVA/CECS) NFs through the electrospinning method. Their findings revealed that the PVA/CECS electrospun NFs were non-toxic to L929 cells and had the potential as a wound dressing[76]. Additionally, another study was conducted to create a new wound dressing using PVA/CS/Starch electrospun nanofibrous mats. Results from MTT testing demonstrated that the electrospun PVA/CS/Starch nanofibrous mats effectively promoted cell growth and proliferation, verifying their biocompatibility for wound dressings[5].

This study utilizedCNF membranes to investigate cell adhesion, spreading, and interaction. The fibroblasts were observed to have adhered and migrated on the surface of the CNFs, indicating the high biocompatibility of all fibers. Furthermore, it was observed that the incorporation of Vit E augmented cellular adhesion and proliferation. Comparable discoveries were reported by Sheng et al., who investigated the effect of novel Vit E -loaded silk fibroin (SF) nanofibrous mats on the spread and proliferation of mouse skin fibroblasts (L929 cells). The study demonstrated that the inclusion of Vit E-TPGS in SF nanofibrous mats increased their ability to shield cells from oxidative stress caused by tert-butyl hydroperoxide[77].

The cell attachment study for the CNF and CNF + Vit E samples demonstrated that fibroblast cells attach to the nanofibrous mat properly and formed a continuous layer over the NFs as an artificial ECM. The attached cells had spindle like structure and proliferate well over the NFs. These observations confirm the cytocompatibility of the prepared samples.

Regarding the hemolysis assay, the results of our study have been deemed a safe hemostatic material according to the American Society for Testing and Materials (ASTM F 756–00, 2000)[78].

Totally, conventional dressings (such as cotton and gauze) are cost-effective and absorbent but passively isolate wounds. However, they may cause dehydration and discomfort due to increased adhesion. Biomedical wound dressings (natural, synthetic) offer advantages like moisture absorption and minimal tissue adhesion, along with inherent antibacterial properties. Synthetic polymers such as PVA have good mechanical properties but lack cell binding sites. In contrast, natural materials such as Gel, CS demonstrate excellent biocompatibility, promoting tissue regeneration. These natural dressings outperform traditional options, providing superior

permeability while resisting bacterial invasion. Natural biomaterials, despite their unique properties, face limitations in mechanical strength[79]. This study effectively produced PVA/CS/Ze/Gel/Vit E nanofibrous scaffolds with the mean size of 203 nm via dual-opposite electrospinning for wound healing. These NFs resemble the ECM structure, enhancing tissue regeneration.

Conclusion

This study effectively produced PVA/CS/Ze/Gel/Vit E nanofibrous scaffolds via dual-opposite electrospinning for wound healing. The scaffolds were subject to characterization and were identified to exhibit enhanced cellular performance and inherent biocompatibility. In addition, produced NFs possess desirable properties such as biodegradability, flexibility, biocompatibility, hydrophilicity, and anti-bacterial activity. These specific properties render them well-suited for application as ulcer dressings to expedite skin ulcer regeneration and healing. However, there are crucial steps should be addressed such as in vivo studies for safety, long-term stability, and clinical trials.

Data availability

The datasets generated during and/or analysed during the current study are available from the corresponding author on reasonable request.

Received: 20 May 2024; Accepted: 30 September 2024
Published online: 11 October 2024

References

1. El Ayadi, A., Jay, J. W. & Prasai, A. Current approaches targeting the wound healing phases to attenuate fibrosis and scarring. *Int. J. Mol. Sci.* **21**, 1105 (2020).
2. Chen, M. et al. Dynamic covalent constructed self-healing hydrogel for sequential delivery of antibacterial agent and growth factor in wound healing. *Chem. Eng. J.* **373**, 413–424 (2019).
3. Fahimirad, S. & Ajalloueian, F. Naturally-derived electrospun wound dressings for target delivery of bio-active agents. *Int. J. Pharm.* **566**, 307–328 (2019).
4. Esmaeili Abdar, Z., Jafari, R., Mohammadi, P. & Nadri, S. The optimal electrical stimulation for neural differentiation of conjunctiva mesenchymal stem cells. *Int. J. Artif. Organs.* **45**, 695–703 (2022).
5. Adeli, H., Khorasani, M. T. & Parvazinia, M. Wound dressing based on Electrospun PVA/chitosan/starch nanofibrous mats: fabrication, antibacterial and cytocompatibility evaluation and in vitro healing assay. *Int. J. Biol. Macromol.* **122**, 238–254 (2019).
6. Farhaj, S., Conway, B. R. & Ghori, M. U. Nanofibres in drug delivery applications. *Fibers.* **11**, 21 (2023).
7. Alven, S., Peter, S., Mbese, Z. & Aderibigbe, B. A. Polymer-based wound dressing materials loaded with bioactive agents: potential materials for the treatment of diabetic wounds. *Polymers.* **14**, 724 (2022).
8. Rodríguez-Rodríguez, R., Espinosa-Andrews, H., Velasquillo-Martínez, C. & García-Carvajal, Z. Y. Composite hydrogels based on gelatin, Chitosan and polyvinyl alcohol to biomedical applications: a review. *Int. J. Polym. Mater. Polym. Biomaterials.* **69**, 1–20 (2020).
9. Abid, S. et al. Investigating alginate and chitosan electrospun nanofibers as a potential wound dressing: an in vitro study. *Nanocomposites.* **10**, 254–267 (2024).
10. Jayakumar, R., Prabaharan, M., Kumar, P. S., Nair, S. & Tamura, H. Biomaterials based on chitin and chitosan in wound dressing applications. *Biotechnol. Adv.* **29**, 322–337 (2011).
11. Gomes, S. R. et al. In vitro and in vivo evaluation of electrospun nanofibers of PCL, chitosan and gelatin: a comparative study. *Mater. Sci. Engineering: C.* **46**, 348–358 (2015).
12. Mohammadi, M. R., Kargozar, S., Bahrami, S. & Rabbani, S. An excellent nanofibrous matrix based on gum tragacanth-poly (Ɛ-caprolactone)-poly (vinyl alcohol) for application in diabetic wound healing. *Polym. Degrad. Stab.* **174**, 109105 (2020).
13. Zhou, Y. et al. Photocrosslinked maleilated chitosan/methacrylated poly (vinyl alcohol) bicomponent nanofibrous scaffolds for use as potential wound dressings. *Carbohydr. Polym.* **168**, 220–226 (2017).
14. Deng, L. et al. Characterization of gelatin/zein nanofibers by hybrid electrospinning. *Food Hydrocoll.* **75**, 72–80 (2018).
15. Naghibzadeh, M. et al. Application of electrospun gelatin nanofibers in tissue engineering. *Biointerface Res. Appl. Chem.* **8**, 3048–3052 (2018).
16. Shukla, R. & Cheryan, M. Zein: the industrial protein from corn. *Ind. Crops Prod.* **13**, 171–192 (2001).
17. Gorham, J. Chemical analysis of Indian corn. *New. Engl. J. Med. Surg. Collateral Branches Sci.* **9**, 320–328 (1820).
18. Paliwal, R. & Palakurthi, S. Zein in controlled drug delivery and tissue engineering. *J. Controlled Release.* **189**, 108–122 (2014).
19. Ullah, A. et al. Clay-corn-caprolactone a novel bioactive clay polymer nanofibrous scaffold for bone tissue engineering. *Appl. Clay Sci.* **220**, 106455 (2022).
20. Li, H. et al. Electrospun gelatin nanofibers loaded with vitamins a and E as antibacterial wound dressing materials. *RSC Adv.* **6**, 50267–50277 (2016).
21. Kheradvar, S. A., Nourmohammadi, J., Tabesh, H. & Bagheri, B. Starch nanoparticle as a vitamin E-TPGS carrier loaded in silk fibroin-poly (vinyl alcohol)-Aloe vera nanofibrous dressing. *Colloids Surf., B.* **166**, 9–16 (2018).
22. Celebioglu, A. & Uyar, T. Antioxidant vitamin E/cyclodextrin inclusion complex electrospun nanofibers: enhanced water solubility, prolonged shelf life, and photostability of vitamin E. *J. Agric. Food Chem.* **65**, 5404–5412 (2017).
23. DeFrates, K. et al. Air-jet spinning corn zein protein nanofibers for drug delivery: Effect of biomaterial structure and shape on release properties. *Mater. Sci. Engineering: C.* **118**, 111419 (2021).
24. Ferreira, C. A. et al. Multifunctional gelatin/chitosan electrospun wound dressing dopped with Undaria Pinnatifida phlorotannin-enriched extract for skin regeneration. *Pharmaceutics.* **13**, 2152 (2021).
25. Zahra, F. T., Quick, Q. & Mu, R. Electrospun PVA fibers for drug delivery: a review. *Polymers.* **15**, 3837 (2023).
26. Balouiri, M., Sadiki, M. & Ibnsouda, S. K. Methods for in vitro evaluating antimicrobial activity: a review. *J. Pharm. Anal.* **6**, 71–79 (2016).
27. Hasan, A. et al. Electrospun scaffolds for tissue engineering of vascular grafts. *Acta Biomater.* **10**, 11–25 (2014).
28. Sobhanian, P., Khorram, M., Hashemi, S. S. & Mohammadi, A. Development of nanofibrous collagen-grafted poly (vinyl alcohol)/gelatin/alginate scaffolds as potential skin substitute. *Int. J. Biol. Macromol.* **130**, 977–987 (2019).
29. Amand, F. K. & Esmaeili, A. Investigating the properties of electrospun nanofibers made of hybride polymer containing anticoagulant drugs. *Carbohydr. Polym.* **228**, 115397 (2020).
30. Manikandan, A., Mani, M. P., Jaganathan, S. K., Rajasekar, R. & Jagannath, M. Formation of functional nanofibrous electrospun polyurethane and murivenna oil with improved haemocompatibility for wound healing. *Polym. Test.* **61**, 106–113 (2017).

31. Varma, R. & Vasudevan, S. Extraction, characterization, and antimicrobial activity of chitosan from horse mussel modiolus modiolus. *ACS Omega*. **5**, 20224–20230 (2020).
32. Agarwal, M. et al. Preparation of Chitosan nanoparticles and their in-vitro characterization. *Int. J. Life-Sciences Sci. Res.* **4**, 1713–1720 (2018).
33. Qashou, S. I., El-Zaidia, E., Darwish, A. & Hanafy, T. Methylsilicon phthalocyanine hydroxide doped PVA films for optoelectronic applications: FTIR spectroscopy, electrical conductivity, linear and nonlinear optical studies. *Phys. B: Condens. Matter*. **571**, 93–100 (2019).
34. Alrowaili, Z., Taha, T., El-Nasser, K. S. & Donya, H. Significant enhanced optical parameters of PVA-Y 2 O 3 polymer nanocomposite films. *J. Inorg. Organomet. Polym Mater.* **31**, 3101–3110 (2021).
35. Kadry, G. Comparison between gelatin/carboxymethyl cellulose and gelatin/carboxymethyl nanocellulose in tramadol drug loaded capsule. *Heliyon.* **5**, e02404 (2019).
36. da Almeida, P. F., da Silva Lannes, S. C., Calarge, F. A., da Brito Farias, T. M. & Santana, J. C. C. FTIR characterization of gelatin from chicken feet. *J. Chem. Chem. Eng.* **6**, 1029 (2012).
37. Hussain, K., Aslam, Z., Ullah, S. & Shah, M. R. Synthesis of pH responsive, photocrosslinked gelatin-based hydrogel system for control release of ceftriaxone. *Chem. Phys. Lipids*. **238**, 105101 (2021).
38. Hassan, N., Ahmad, T., Zain, N. M. & Awang, S. R. Identification of bovine, porcine and fish gelatin signatures using chemometrics fuzzy graph method. *Sci. Rep.* **11**, 9793 (2021).
39. Sadeghinia, A., Soltani, S., Aghazadeh, M., Khalilifard, J. & Davaran, S. Design and fabrication of clinoptilolite–nanohydroxyapatite/chitosan–gelatin composite scaffold and evaluation of its effects on bone tissue engineering. *J. Biomedical Mater. Res. Part. A*. **108**, 221–233 (2020).
40. Schmitz, F., de Albuquerque, M. B. S., Alberton, M. D., Riegel-Vidotti, I. C. & Zimmermann, L. M. Zein films with ZnO and ZnO: mg quantum dots as functional nanofillers: new nanocomposites for food package with UV-blocker and antimicrobial properties. *Polym. Test.* **91**, 106709 (2020).
41. Esnaashari, S. S., Muhammadnejad, S., Amanpour, S. & Amani, A. A combinational approach towards treatment of breast cancer: an analysis of noscapine-loaded polymeric nanoparticles and doxorubicin. *AAPS PharmSciTech*. **21**, 1–12 (2020).
42. Fadeikina, I., Peunkova, E. & Zuev, B. Determination of vitamin E (α-tocopherol acetate) on the surface of human skin by IR Fourier-transform spectrometry and study of some aspects of its transdermal transfer. *J. Anal. Chem.* **76**, 191–195 (2021).
43. Lin, S. J. & Pascall, M. A. Incorporation of vitamin E into chitosan and its effect on the film forming solution (viscosity and drying rate) and the solubility and thermal properties of the dried film. *Food Hydrocoll.* **35**, 78–84 (2014).
44. Yeamsuksawat, T. & Liang, J. Characterization and release kinetic of crosslinked chitosan film incorporated with α-tocopherol. *Food Packaging Shelf Life*. **22**, 100415 (2019).
45. Martins, J. T., Cerqueira, M. A. & Vicente, A. A. Influence of α-tocopherol on physicochemical properties of chitosan-based films. *Food Hydrocoll.* **27**, 220–227 (2012).
46. Tonkin, M., Khan, S., Wani, M. Y. & Ahmad, A. Quorum Sensing-A stratagem for conquering multi-drug resistant pathogens. *Curr. Pharm. Design*. **27**, 2835–2847 (2021).
47. Baker, S., Pasha, A. & Satish, S. Biogenic nanoparticles bearing antibacterial activity and their synergistic effect with broad spectrum antibiotics: emerging strategy to combat drug resistant pathogens. *Saudi Pharm. J.* **25**, 44–51 (2017).
48. Worthington, R. J. & Melander, C. Combination approaches to combat multidrug-resistant bacteria. *Trends Biotechnol.* **31**, 177–184 (2013).
49. Sharma, G. K. & James, N. R. *In Recent Developments in Nanofibers Research* (IntechOpen, 2022).
50. Liu, Y. et al. Advances in the Preparation of Nanofiber Dressings by Electrospinning for promoting Diabetic Wound Healing. *Biomolecules*. **12**, 1727 (2022).
51. Keshvardoostchokami, M. et al. Electrospun nanofibers of natural and synthetic polymers as artificial extracellular matrix for tissue engineering. *Nanomaterials*. **11**, 21 (2020).
52. Ignatova, M., Manolova, N. & Rashkov, I. Electrospun Antibacterial Chitosan-B ased fibers. *Macromol. Biosci.* **13**, 860–872 (2013).
53. Iacob, A. T. et al. An overview of biopolymeric electrospun nanofibers based on polysaccharides for wound healing management. *Pharmaceutics*. **12**, 983 (2020).
54. Zhu, L., Liu, X., Du, L. & Jin, Y. Preparation of asiaticoside-loaded coaxially electrospinning nanofibers and their effect on deep partial-thickness burn injury. *Biomed. Pharmacother.* **83**, 33–40 (2016).
55. Dorati, R. et al. Study on hydrophilicity and degradability of chitosan/polylactide-co-polycaprolactone nanofibre blend electrospun membrane. *Carbohydr. Polym.* **199**, 150–160 (2018).
56. Ohkawa, K., Cha, D., Kim, H., Nishida, A. & Yamamoto, H. Electrospinning of Chitosan. *Macromol. Rapid Commun.* **25**, 1600–1605 (2004).
57. Jia, Y. T. et al. Fabrication and characterization of poly (vinyl alcohol)/chitosan blend nanofibers produced by electrospinning method. *Carbohydr. Polym.* **67**, 403–409 (2007).
58. Adibzadeh, S., Bazgir, S. & Katbab, A. A. Fabrication and characterization of chitosan/poly (vinyl alcohol) electrospun nanofibrous membranes containing silver nanoparticles for antibacterial water filtration. *Iran. Polym. J.* **23**, 645–654 (2014).
59. Magana, M. et al. Options and limitations in clinical investigation of bacterial biofilms. *Clin. Microbiol. Rev.* **31**, 101128cmr00084–101128cmr00016 (2018).
60. Haider, A., Haider, S. & Kang, I. K. A comprehensive review summarizing the effect of electrospinning parameters and potential applications of nanofibers in biomedical and biotechnology. *Arab. J. Chem.* **11**, 1165–1188 (2018).
61. Vilchez, A., Acevedo, F., Cea, M., Seeger, M. & Navia, R. Applications of electrospun nanofibers with antioxidant properties: a review. *Nanomaterials*. **10**, 175 (2020).
62. Fathi, M., Nasrabadi, M. N. & Varshosaz, J. Characteristics of vitamin E-loaded nanofibres from dextran. *Int. J. Food Prop.* **20**, 2665–2674 (2017).
63. Kalantary, S., Golbabaei, F., Latifi, M., Shokrgozar, M. A. & Yaseri, M. Feasibility of using vitamin E-loaded poly (ε-caprolactone)/gelatin nanofibrous mat to prevent oxidative stress in skin. *J. Nanosci. Nanotechnol.* **20**, 3554–3562 (2020).
64. Nguyen, H. M., Le, T. T. N., Nguyen, A. T., Le, H. N. T. & Pham, T. T. Biomedical materials for wound dressing: recent advances and applications. *RSC Adv.* **13**, 5509–5528 (2023).
65. Nosrati, H. et al. Nanocomposite scaffolds for accelerating chronic wound healing by enhancing angiogenesis. *J. Nanobiotechnol.* **19**, 1–21 (2021).
66. Bazmandeh, A. Z., Mirzaei, E., Fadaie, M., Shirian, S. & Ghasemi, Y. Dual spinneret electrospun nanofibrous/gel structure of chitosan-gelatin/chitosan-hyaluronic acid as a wound dressing: In-vitro and in-vivo studies. *Int. J. Biol. Macromol.* **162**, 359–373 (2020).
67. Kim, M. S., Park, S. J., Gu, B. K. & Kim, C. H. Fabrication of chitosan nanofibers scaffolds with small amount gelatin for enhanced cell viability. *Appl. Mech. Mater.* **749**, 220–224 (2015).
68. Wang, D. et al. Fabrication and characterization of gelatin/zein nanofiber films loading perillaldehyde for the preservation of chilled chicken. *Foods*. **10**, 1277 (2021).
69. Pollack, S. V. & Wound Healing A review: II. Environmental factors affecting Wound Healing. *J. Dermatol. Surg. Oncol.* **5**, 477–481 (1979).
70. Jones, J. Winter's concept of moist wound healing: a review of the evidence and impact on clinical practice. *J. Wound Care*. **14**, 273–276 (2005).

71. Nuutila, K. & Eriksson, E. Moist wound healing with commonly available dressings. *Adv. Wound Care*. **10**, 685–698 (2021).
72. Alven, S. & Aderibigbe, B. A. Fabrication of Hybrid nanofibers from Biopolymers and Poly (Vinyl Alcohol)/Poly (ε-Caprolactone) for wound dressing applications. *Polymers*. **13**, 2104 (2021).
73. Christopherson, G. T., Song, H. & Mao, H. Q. The influence of fiber diameter of electrospun substrates on neural stem cell differentiation and proliferation. *Biomaterials*. **30**, 556–564 (2009).
74. Haycock, J. W. 3D cell culture: a review of current approaches and techniques. *3D cell culture: methods and protocols*, 1–15 (2011).
75. Kuo, C. W., Chueh, D. Y. & Chen, P. Investigation of size–dependent cell adhesion on Nanostructured interfaces. *J. Nanobiotechnol.* **12**, 1–10 (2014).
76. Zhou, Y. et al. Electrospun water-soluble carboxyethyl chitosan/poly (vinyl alcohol) nanofibrous membrane as potential wound dressing for skin regeneration. *Biomacromolecules*. **9**, 349–354 (2008).
77. Sheng, X. et al. Vitamin E-loaded silk fibroin nanofibrous mats fabricated by green process for skin care application. *Int. J. Biol. Macromol.* **56**, 49–56 (2013).
78. ASTM, F. 756-00. Standard practice for assessment of hemolytic properties of materials. *Philadelphia: Am. Soc. Test. Mater.* (2000).
79. Wang, F., Hu, S., Jia, Q. & Zhang, L. Advances in electrospinning of natural biomaterials for wound dressing. *Journal of Nanomaterials*. **2020**, 8719859 (2020).

Acknowledgements

This research was supported by Tehran University of Medical Sciences, Grant No. 1401-2-148-58905.

Authors' contributions

Homa Hodaei: Methodology, Investigation, Zahra Esmaeili: Writing – original draft. Yousef Erfani: Conceptualization, Methodology. Seyedeh Sara Esnaashari: Conceptualization, Methodology, Writing – review & editing, Supervision. Mahvash Garavand: Investigation. Mahdi Adabi: Writing – review & editing, Supervision.

Declarations

Competing interests

The authors declare no competing interests.

Additional information

Correspondence and requests for materials should be addressed to S.S.E. or M.A.

Reprints and permissions information is available at www.nature.com/reprints.

Publisher's note Springer Nature remains neutral with regard to jurisdictional claims in published maps and institutional affiliations.